Z. Angew. Math. Phys. 63 (2012), 905–919

0044-2275/12/050905-15
published online April 17, 2012
DOI 10.1007/s00033-012-0211-2

Zeitschrift für angewandte Mathematik und Physik ZAMP

Stokes flow between eccentric rotating spheres with slip regime

M. S. Faltas and E. I. Saad

Abstract. The steady axisymmetric flow problem of a viscous fluid contained between two eccentric spheres that rotate about an axis joining their centers with different angular velocities is considered. A linear slip of Basset-type boundary condition at both surfaces of the spherical particle and the container is used. Under the Stokesian assumption, a general solution is constructed from the superposition of basic solutions in the spherical coordinate systems based on the inner solid particle and the spherical container. The boundary conditions on the particle's surface and spherical container are satisfied by a collocation technique. Numerical results for the coupling coefficient acting on the particle are obtained with good convergence for various values of the ratio of particle-to-container radii, the relative distance between the centers of the particle and container, the slip coefficients and the relative angular velocity. In the limiting cases, the numerical values of the coupling coefficient for the solid sphere in concentric position with the container and when the particle is near the inner surface of the container are obtained, and the results are in good agreement with the available values in the literature. The variation of the coupling coefficient with respect the parameters considered are tabulated and displayed graphically.

Mathematics Subject Classification. 76A05.

Keywords. Stokes flow · Eccentric spheres · Slip condition · Normalized coupling coefficient.

1. Introduction

The area of research studying rotating fluid systems have been and continue to be a very important part in fluid mechanics, since all fluid phenomena in practice involve rotation to some extent. Among various rotating fluid systems, the motion of a viscous fluid contained between two concentric rotating spheres is of specific interest in both engineering design and geophysics because of its wide application in different fields, for example, centrifuges, fluid gyroscopes Pedlosky [1] and colloidal science [2–6].

One of the important physical quantities, which is needed in different applications, is the couple experienced on the rotating bodies by the fluid. Therefore, many attempts have been made to evaluate such couple for various bodies of revolution. When inertial effects can be validly ignored, so Stokes's linearized theory applies, the solutions have been found for some configurations, for example, a sphere Lamb [7], spheroids, pair of spheres and a circular disk Jeffery [8], and a spindle, a torus, and a lens Kanwal [9], and problems for asymmetric translation and rotation of two spheres [10–12]. This value of the couple is needed in designing and calibrating viscometries, and better predictions of couple are essential in order to improve the accuracy of viscosity measurements. Landau and Lifshitz [13] discussed the slow motion of fluid contained in the space between two concentric spheres. Munson and Joseph [14] also investigated the problem of steady motion of a viscous fluid contained between two concentric spheres that rotate about a common axis with different angular velocities and allowing for the inertia term. The resulting flow pattern and the couple required to rotate the spheres are presented for various values of the Reynolds numbers. Munson [15] solves perturbatively the case where the spheres are displaced along their common axis, so that they are eccentric but remain coaxial. O'Neill and Majumdar [16,17] have discussed the problem of asymmetrical slow viscous fluid motions caused by the translation or rotation of two spheres.

They found the exact solutions for any values of the ratio of radii and separation parameters. Cooley [18] has investigated the problem of fluid motion generated by a sphere rotating close to a fixed sphere about a diameter perpendicular to the line of centers in the case when the motion is sufficiently slow to permit the linearized of the Navier–Stokes equations by neglecting the inertia terms. He used a method of matched asymptotic expansions to find asymptotic expressions for the forces and couples acting on the spheres as the minimum clearance between them tends to zero. Kamel and Chan Man Fong [19] have investigated the steady flow of a micropolar fluid flow between two eccentric coaxially rotating spheres using perturbation techniques.

Recently, the problem of concentric pervious spheres carrying a fluid source at their center and rotating slowly with different uniform angular velocities about a diameter has been studied by Srivastava [20]. Shankar [21] suggested a general method for deriving exact solutions to the Stokes flow in and around a sphere and between two concentric spheres, which are generated by meridional driving on the spherical boundaries. A numerical study of flow and heat transfer between two rotating spheres has been done by Jabari Moghadam and Rahimi [22] in which the fluid contained between two vertically eccentric spheres maintained at different temperature and rotating about a common axis with different angular velocities when the angular velocities are arbitrary functions of time. Liu and Prosperetti [23] numerically studied several effects of neighboring boundaries on the steady flow induced by a rotating sphere in various configurations. They found that, in these conditions, the flow exhibits an interesting and perhaps unexpected richness under the action of the competing action of centrifugal, inertial and viscous effects. The system of spherical particle moving inside a spherical cavity can be taken as an idealized model for the capture of particles in filters composed of connecting pores. The hydrodynamic interaction between the particle and the cavity wall determines the deposition behavior of the particle toward the wall and thus relates closely to the capture efficiency of the filter [24].

The Navier–Stokes equations of fluid flow are typically solved under no-slip boundary conditions, that is, assuming that the layer of liquid next to a solid surface moves with the local velocity of the surface. The no-slip condition was a characterized issue in the early development of fluid mechanics. Experimental observations appeared to confirm its validity over a vast array of differing situations. However, in the last century, several studies have shown that this condition might not always hold and that fluid slippage might occur at the solid boundary [25–27]. O'Neill et al. [28] used a linear slip, Basset-type [29], boundary condition to remove the contact-line singularity that would otherwise prevent the movement of a half-submerged sphere normal to a planner free surface bounding a semi-infinite viscous fluid. In fact, nearly 200 years ago, Navier [30] proposed a general boundary condition that permits the possibility of fluid slip at a solid boundary. This boundary condition assumes that the tangential velocity of the fluid relative to the solid at a point on its surface is proportional to the tangential stress acting at that point. Basset [29] derived expressions for the force and couple exerted by the fluid on a translating and rotating rigid sphere with a slip boundary condition at its surface (e.g., a settling aerosol sphere). Later, the quasisteady translation and steady rotational of a slip spherical particle in a slip spherical cavity are also theoretically studied in [31]. Tekasakul et al. [32] have numerically studied the torques and local stresses on two axisymmetric particles rotating (rotate with the same frequency and in the same direction about a common axis of symmetry) in a viscous fluid with slip boundary conditions at the particle surfaces using the Green's function technique.

While the solutions of the Stokesian flow equations with slip conditions are of substantial interest for gases, recently, it has been noted that slip conditions are of interest for liquids as well, particularly with respect to microscopic sense. Neto et al. [33] provide an excellent review of experimental studies regarding the phenomenon of slip of Newtonian fluids at solid interface. They give a particular attention to the factors that have effect on the fluid slippage at the solid boundary, as surface roughness, wetability and the presence of gaseous layers might have on the measured interfacial slip. In recent years, there has been an increased interest in using the slip boundary condition for Newtonian fluids [34,35], for Poiseuille flow [38] and for micropolar and microstretch fluids [36,37].

The boundary collocation method has been used by many authors to solve flow problems in viscous fluids. Gluckman et al. [39] developed truncated series boundary collocation method to study the unbounded axisymmetric multispherical Stokes flow. The theoretically predicated drag results are in good agreement with experimentally measured values. Later, Leichtberg et al. [40] extended the work of Gluckman et al. [39] to bounded flows for coaxial chains of spheres in a tube. Ganatos et al. [41,42] modified the collocation series solution techniques to investigate the Stokes flow of perpendicular and parallel motion of a sphere between two parallel plane boundaries. The collocation method has been also used to treat the axisymmetric slip-flow problems, for example, [43–45]. Recently, Keh and Lee [24] employed the boundary collocation technique to examine the axisymmetric motion of a spherical particle with a slip surface in a nonconcentric spherical cavity. Faltas and Saad [46] have provided results of an analytical/numerical study of quasisteady Stokes flow past an assemblage of spherical particles. The approach is based on a particle-in-cell model. Such containers are used in engineering designs, such as centrifuges and fluid gyroscopes, and are important in geophysics. The authors use an analytical method combined with a boundary collocation technique in order to solve the Stokes equations corresponding to the fluid flow region.

This paper presents the solution of the Stokes' flow of an incompressible and steady viscous fluid contained between two eccentric (two centers do not coincide with each other) spheres that rotate about a line joining their centers with different uniform angular velocities. This spherical eccentric annulus flow is a special example of fluid motion in a rotating container and is of interest in both engineering design and geophysics. The fluid is allowed to slip frictionally at both the spherical inner particle and outer container surfaces. A combined analytical/numerical method with the boundary collocation technique has been used to solve the Stokes equations for the fluid flow field. The rotational couple coefficient acting on the particle is obtained with good convergence for various parameters considered. In addition, some numerical results, which refer to the case of a solid sphere concentric with the external cell surface, are also included. These results are compared with those corresponding to the case of the sphere located near the cell surface with small curvature.

2. Statement of the problem

We consider here the steady motion of an incompressible viscous fluid of viscosity μ filling the gap between two eccentric spheres that are of radii a and b and rotate about a common axis joining their centers with constant angular velocities Ω_1 and Ω_2. The geometry of the spherical eccentric annulus considered is indicated in Fig. 1. The fluid is allowed to slip frictionally at particle and container surfaces. Here, (ρ, ϕ, z) and (r_2, θ_2, ϕ) denote the circular cylindrical and spherical coordinate systems, respectively, with the origin of coordinates at the center of the container. The center of the particle is located away from the container center at a distance d, where (r_1, θ_1, ϕ) are the spherical coordinates based on the center of the spherical particle, and the relation between r_1 and r_2 is given by $r_1^2 = r_2^2 + d^2 - 2\,r_2 d\cos\theta_2$ or by $r_2^2 = r_1^2 + d^2 + 2\,r_1 d\cos\theta_1$. Since the angular velocity is supposed to be small, the assumption of the Stokesian flow may be used. Under these circumstances, the flow is axially symmetric, and all the flow functions are independent of ϕ. Thus, we choose $\vec{q}$, in cylindrical coordinates, in the form

$$\vec{q} = q_\phi(r, \theta)\,\vec{e}_\phi. \tag{2.1}$$

The fluid flow between the particle and the container is governed by the Stokes equations

$$\nabla \cdot \vec{q} = 0, \tag{2.2}$$

$$\nabla p - \mu\,\nabla^2 \vec{q} = 0. \tag{2.3}$$

From the set of equations, we have the following

$$\frac{\partial p}{\partial \rho} = 0, \qquad \frac{\partial p}{\partial z} = 0, \tag{2.4}$$

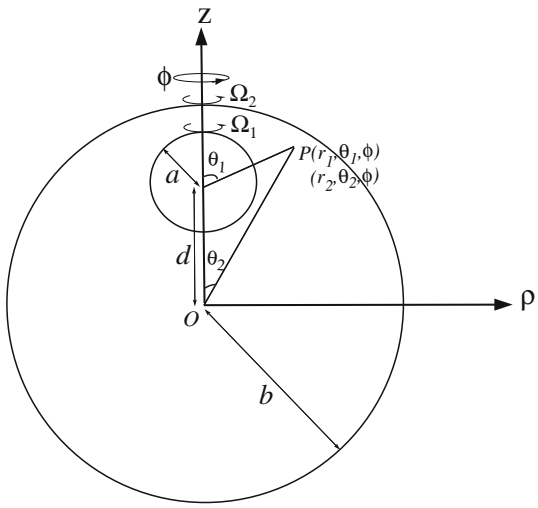

FIG. 1. The physical situation and the description of the coordinate systems

$$L\, q_\phi = 0, \tag{2.5}$$

where L is the axisymmetric Stokesian operator

$$L = \nabla^2 - \frac{1}{\rho^2} = \frac{\partial^2}{\partial \rho^2} + \frac{1}{\rho}\frac{\partial}{\partial \rho} + \frac{\partial^2}{\partial z^2} - \frac{1}{\rho^2}. \tag{2.6}$$

Equation (2.4) gives a constant pressure p throughout the flow region. To solve Eq. (2.5), which is equivalent to the Stokes equations of a viscous fluid (2.2) and (2.4), the boundary conditions have to be specified.

At the particle surface $r_1 = a$ and container surface $r_2 = b$, we shall assume slip and use the most likely hypothesis [2,29]; the fluid velocity at the particle and container surfaces become

$$q_\phi = \Omega_1\, r_1\, \sin\theta_1 + \frac{1}{\beta_1}\, t_{r_1\phi}, \quad r_1 = a, \tag{2.7}$$

$$q_\phi = \Omega_2\, r_2\, \sin\theta_2 - \frac{1}{\beta_2}\, t_{r_2\phi}, \quad r_2 = b, \tag{2.8}$$

where $t_{r_i\phi}$ with $i = 1, 2$ is the shear stress for the flow, and the coefficient, β_i, is termed as the coefficient of sliding friction. The coefficient β_i is a measure of the degree of tangential slip existing between the fluid and solid at its surface. It is assumed to depend only on the nature of the fluid and solid surface. It might depend on some other parameters like strain rate [47]. Throughout this work, both the slip coefficients (β_1 and β_2) are taken to be constant. In the limiting case of $\beta_1 = 0$, there is a perfect slip at the surface of the sphere, and the solid sphere acts like a spherical gas bubble, while the standard no-slip boundary condition for solids is obtained by letting $\beta_i \to \infty$.

3. Method of solution

A solution to Eq. (2.5) suitable for satisfying boundary conditions on the spherical surfaces for the velocity function and the shear stress $t_{r_i\phi}$ in the spherical coordinates is given by

$$q_\phi = a\,\Omega_1 \sum_{n=1}^{\infty} \left[A_n\, r_1^{-n-1}\, P_n^1(\cos\theta_1) + B_n\, r_2^n\, P_n^1(\cos\theta_2)\right], \tag{3.1}$$

$$t_{r_i\phi} = \mu\,\Omega_1 \sum_{n=1}^{\infty} \left[- A_n\,(n+2)\, r_1^{-n-2}\, P_n^1(\cos\theta_1) + B_n\,(n-1)\, r_2^{n-1}\, P_n^1(\cos\theta_2)\right], \tag{3.2}$$

where P_n^1 is the associated Legendre function of order n. The coefficients A_n and B_n are unknown constants that will be determined using the boundary conditions at the particle and cell surfaces. In the expressions (3.1) and (3.2) and in all subsequent expressions in this paper, r_i are nondimensional with respect to the particle surface radius a.

To determine the unknown constants A_n and B_n, we apply the boundary conditions (2.7) and (2.8); one obtains

$$1 = \sum_{n=1}^{\infty} \left\{A_n\, a_{1n}(a,\theta_1) + \left[B_n\, b_{1n}(r_2,\theta_2)\right]_{r_1=a}\right\}, \tag{3.3}$$

$$\Omega = \sum_{n=1}^{\infty} \left\{\left[A_n\, a_{2n}(r_1,\theta_1)\right]_{r_2=b} + B_n\, b_{2n}(b,\theta_2)\right\}, \tag{3.4}$$

where $\Omega = \Omega_2/\Omega_1$ is the relative rotational velocity of the spheres, and the expressions for a_{in} and b_{in} are given in Appendix A. To determine the fluid velocity, the boundary conditions (3.3) and (3.4) should be satisfied exactly along the surface of particle and container surface. This would result in infinite linear algebraic equations for infinite unknown coefficients, which are impossible to be solved. This difficulty can be avoided by the use of a multipole collocation technique [24,39,44]. It requires first that the infinite series be truncated after certain terms so that the number of the unknown coefficients becomes finite. Then, sufficient points on each of the particle surface and container surface are selected as collocation points, where the boundary conditions are enforced to give the same number of linear equations as that of the coefficients. Solving these equations subsequently enables one to determine the flow field. In general, more boundary collocation points are required to attain a given accuracy when the ratio of particle-to-container radii, η, is close to unity and when the relative distance between the centers of the particle and container is also close to unity.

The hydrodynamic couple (in the z direction) exerted on the rotating sphere in a container about the line connecting their centers by the external fluid is obtained from the surface stress tensor t_{ij} as

$$T_z = \int_S \vec{r} \wedge (\vec{n}\cdot\mathbf{t})\cdot\vec{k}\,\mathrm{d}S,$$

where $\vec{r} = a\,\vec{e}_r$, $\vec{n} = \vec{e}_r$ and $\vec{k}$ is the unit vector in the direction of the axis of rotation, and taking the integral over the boundary of the solid surface, we have

$$T_z = 2\,\pi\,a^3 \int_0^{\pi} r^3\, t_{r\phi}|_{r=1} \sin^2\theta\,\mathrm{d}\theta = -8\,\pi\,\mu\,\Omega_1\,a^3\,A_1. \tag{3.5}$$

The above expression shows that only the lowest-order coefficient A_1 contributes to the hydrodynamic couple acting on the particle. This leading coefficient normally is the most accurate (fastest convergent) result obtainable from the boundary collocation technique.

For comparison purposes, we note that for the case where the container surface is absent as $a/(b-d) = 0$, so that the fluid is infinite. The expression for the hydrodynamic couple acting on a rotating rigid sphere with a slip-flow boundary condition at its surface in a viscous fluid at rest at infinity is obtained by Basset [29] as

$$T_z^{\infty} = -8\,\pi\,a^3\,\Omega_1\,\mu\,\frac{\lambda_1}{\lambda_1+3}. \tag{3.6}$$

where $\lambda_1 = \beta_1\,a/\mu$.

The coupling coefficient N is defined as the ratio of the actual hydrodynamic couple experienced by the sphere in the container wall to the couple experienced by a sphere in an infinite expanse of fluid. With the aid of Eqs. (3.5) and (3.6), this becomes

$$N = \frac{T_z}{T_z^{\infty}} = \lambda_1^{-1}\,(\lambda_1+3)\,A_1. \tag{3.7}$$

Note that $N = 1$ as $a/(b-d) = 0$ (the container surface is infinitely far from the particle) for any specified values of β_1 and β_2.

For the slow rotational motion of a solid sphere located at the center of a spherical container, where the fluid may slip at the particle and container surfaces, the exact solution of its normalized hydrodynamic couple was obtained explicitly as (see Appendix B)

$$N = \lambda_2\,(1-\Omega)\,(\lambda_1+3)\left[(3+\lambda_1-\lambda_1\,\eta^3)\,\lambda_2 + 3\eta^4\,\lambda_1\right]^{-1}, \tag{3.8}$$

where $\eta = a/b$ and $\lambda_2 = \beta_2\,a/\mu$. If the outer spherical container is stationary, $\Omega = 0$ (or $\Omega_2 = 0$), that is, we have simply a sphere rotating in a stationary spherical envelope with slip at both surfaces. In this case, expression (3.8) reduces to

$$N = \lambda_2\,(\lambda_1+3)\left[(3+\lambda_1-\lambda_1\,\eta^3)\,\lambda_2 + 3\eta^4\,\lambda_1\right]^{-1}, \tag{3.9}$$

a result obtained by Keh and Chang [31]. It is clear that from (3.8), as $\Omega = 1$, $N = 0$ for any specified values of β_1 and β_2. That is when the particle and the enveloper rotate with the same angular velocities and in the same direction, and the acting couple vanishes.

Here, note that if we consider the limiting case $\lambda_2 \to \infty$, which corresponds to the rotational motion of a slip sphere in a no-slip container, the coupling coefficient is given by

$$N = (\lambda_1+3)\,(1-\Omega)\,(\lambda_1+3-\eta^3\,\lambda_1)^{-1}, \tag{3.10}$$

which reduces to $N = (1-\Omega)\,(1-\eta^3)^{-1}$ as $\lambda_1 \to \infty$.

In the particular case of $\lambda_2 = \lambda_1$, which corresponds to the rotational motion of a sphere located at the center of a concentric spherical container with the same slip coefficient at both spherical surfaces, the coupling coefficient is given by

$$N = (\lambda_1+3)\,(1-\Omega)\left[\lambda_1+3+\eta^3\,(3\eta-\lambda_1)\right]^{-1}. \tag{3.11}$$

The numerical solution of the coupling coefficient, Eq. (3.7), experienced by the axisymmetric motion of a slip spherical particle within a spherical container with slip surface, obtained by using the boundary collocation method described above, is presented here. The systems of linear algebraic equations to be solved for the coefficients A_n and B_n are constructed from Eqs. (3.3) to (3.4).

When specifying the points along the semi-circular generating arcs of the solid sphere and container surfaces where the boundary conditions are exactly satisfied, the first two points that should be chosen are $\theta_i = 0$ and π, since these points control the extreme gaps between the particle and the container surfaces. In addition, the points $\theta_i = \pi/2$ are also important. However, an examination of the systems of linear algebraic equations for the unknown constants A_n and B_n shows that the coefficient matrix becomes singular if these points are used. In order to avoid this singular matrix and achieve good accuracy, we adopt the method recommended in the literature [24,39,41] to choose the collocation points as follows. On the half unit circle $0 \le \theta_i \le \pi$ in any meridional plane, $\theta_i = \varepsilon$, $\pi/2-\varepsilon$, $\pi/2+\varepsilon$ and $\pi-\varepsilon$ are taken as four basic multipoles, where ε is specified by a small value so that the singularities at $\theta_i = 0$, $\pi/2$, and π can be avoided. The other points are selected as mirror-image pairs about $\theta_i = \pi/2$, which are evenly distributed on the two quarter circles, excluding those singularity points. A Gaussian elimination

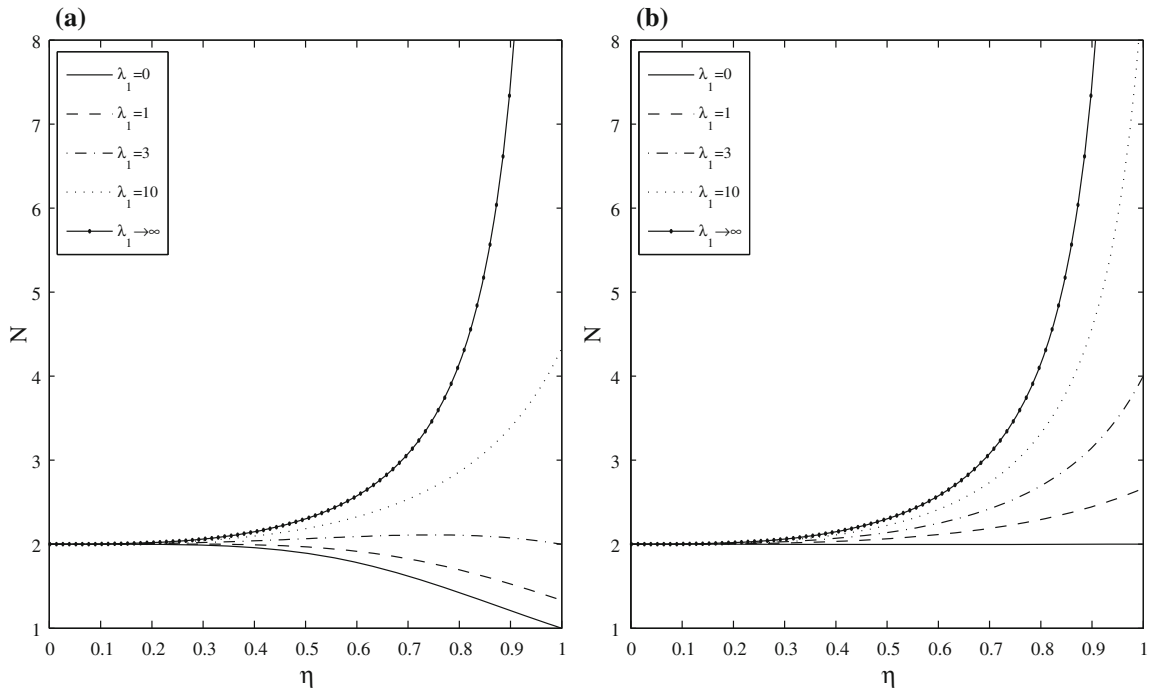

FIG. 2. Variations of the coupling coefficient versus the ratio η for different values of the parameter λ_1 with $\Omega = -1$ and $\delta = 0.25$. **a** and **b** represent the calculations for the $\lambda_2 = \lambda_1$ and $\lambda_2 \to \infty$, respectively

method is used to solve the linear equations to determine the coefficients. The hydrodynamic couple is then calculated.

We present here the collocation solutions of the coupling coefficient N experienced by the rotational motion of a slip spherical particle at an eccentric position in a viscous fluid within a spherical container for various values of the following parameters:

(1) the ratio of the particle-to-container radii, $\eta = a/b$
(2) the relative distance between the centers of the particle and container, $\delta = d/(b-a)$
(3) the slip coefficients of the particle and container surfaces λ_1 and λ_2
(4) the relative angular velocity, $\Omega = \Omega_2/\Omega_1$.

The results are shown in Figs. 2, 3, 4, 5 and 6 and Tables 1, 2 and 3. All results obtained under this collocation method converge to at least six significant figures. For the extreme cases of $\eta = 0.99$ and $\delta = 0.99$, the number of collocation points $N = 80$ is sufficiently large to achieve this convergence.

The normalized hydrodynamic couple, N, is shown as a function of the parameter η in Fig. 2 for the cases of $\lambda_2 = \lambda_1$ and $\lambda_2 \to \infty$ with $\Omega = -1$ and $\delta = 0.25$. It can be seen that, in general, the rotational couple coefficient N increases with the increase in the slip parameters λ_1 and λ_2 for a fixed value of η, which is greater than about 0.3. For values of η, which is less than about 0.3, N is constant ($N \cong 2$) for all values of λ_1 and λ_2.

Figures 2a, 3 and Table 1 indicate, for given values of λ_1 and δ, if $\lambda_2 < 3$, then N decreases monotonically with increasing η, λ_1, and if $\lambda_2 > 3$, then N is monotonic increasing with the increase in η and λ_1. It appears from Fig. 2b and Table 2, in situation with $\lambda_1 = 0$, and $\lambda_2 \to \infty$ (namely, a no-slip envelope is filled with gas bubble that rotates with the same angular velocities but in opposite direction as that of envelope), the value of N is almost 2 for the different values of δ. Figure 4 and Table 3 indicate that when the particle and envelope rotate in opposite directions ($\Omega < 0$), the magnitude of the coupling coefficient

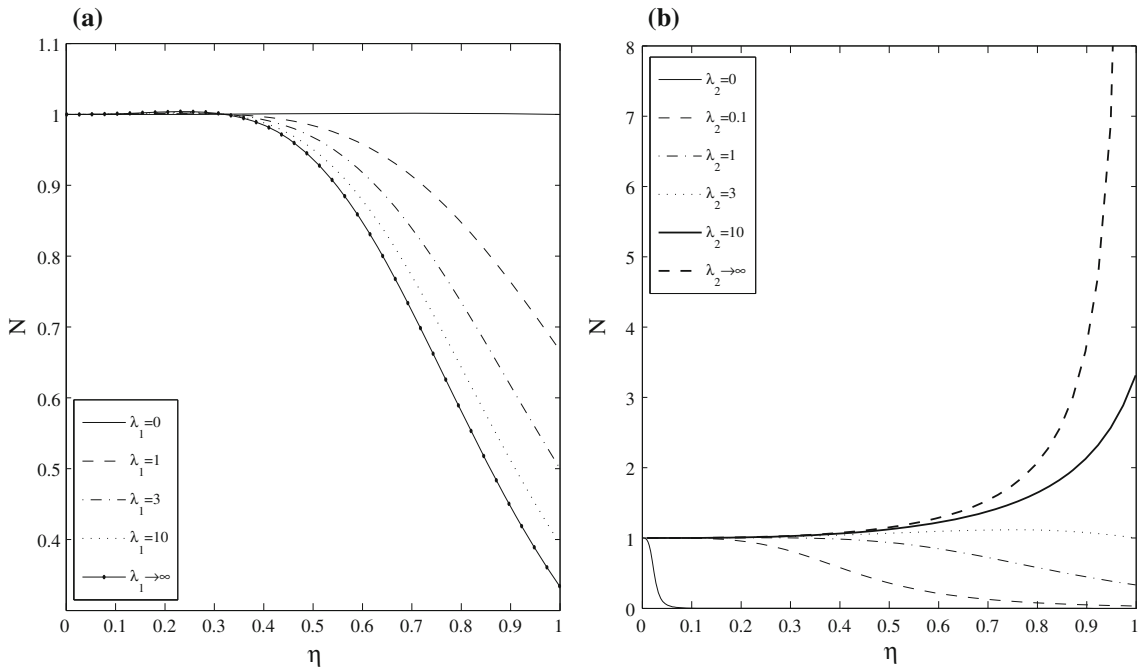

FIG. 3. Variations of the coupling coefficient versus the ratio η for different values of the parameter λ_i with $\Omega = -1$ and $\delta = 0.25$. **a** and **b** represent the calculations for the $\lambda_2 = 1$ and $\lambda_1 \to \infty$, respectively

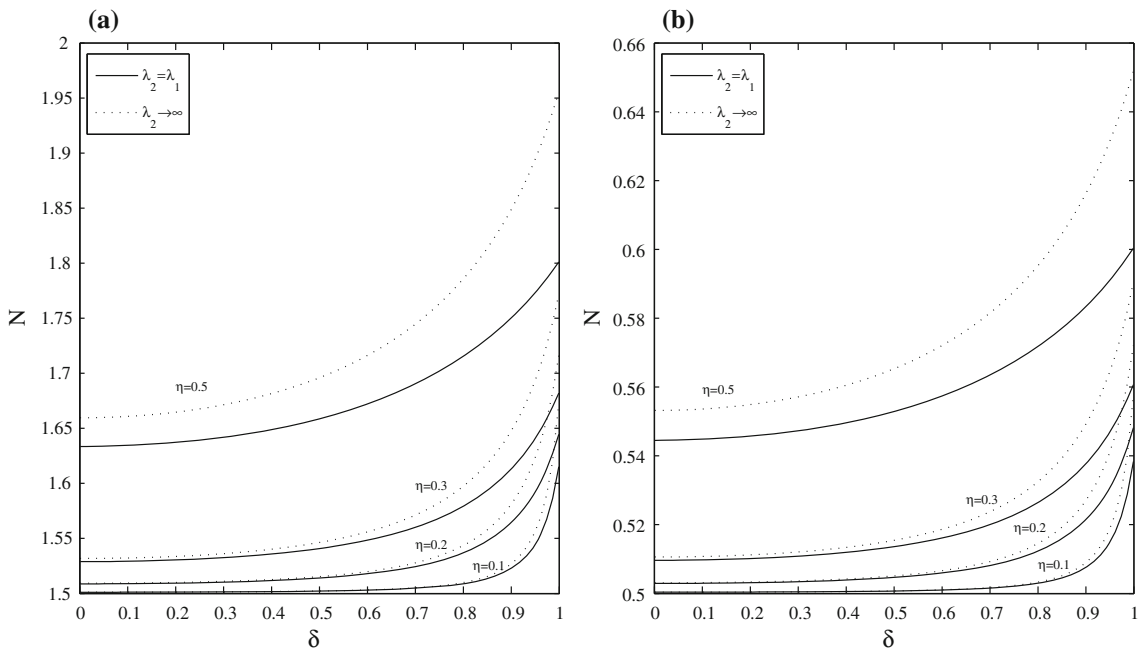

FIG. 4. Variations of the coupling coefficient versus the ratio δ for different values of the parameter η with $\lambda_1 = 10$. **a** and **b** represent the calculations for the $\Omega = -0.5$ and $\Omega = 0.5$, respectively

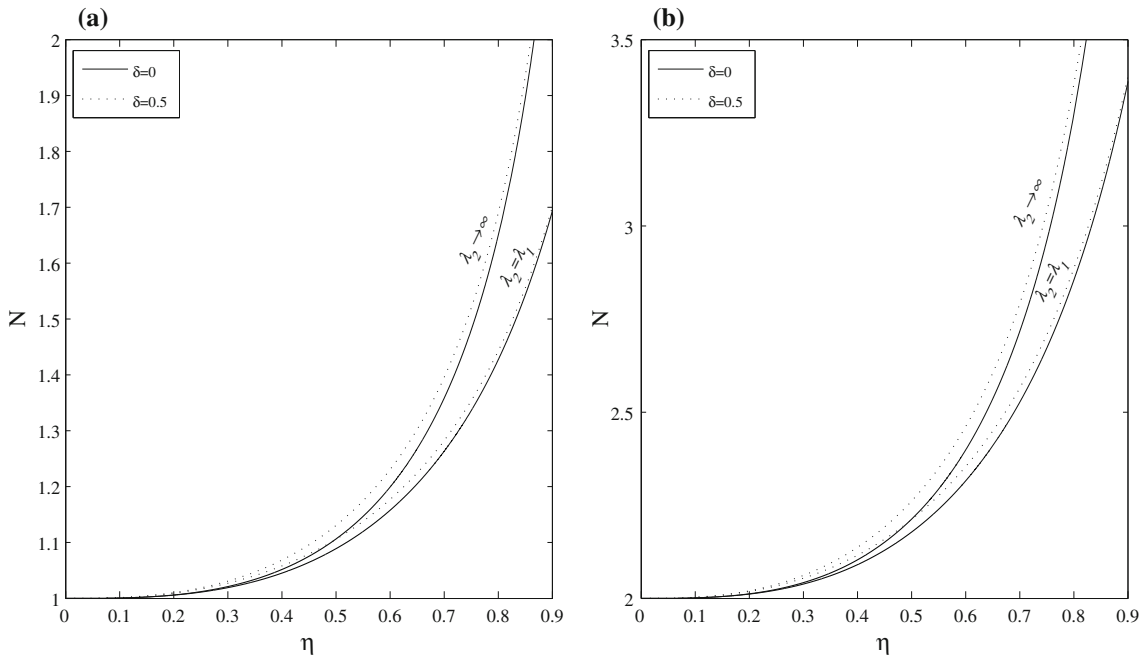

FIG. 5. Variations of the coupling coefficient versus the ratio η for different values of the parameter δ with $\lambda_1 = 10$. **a** and **b** represent the calculations for the $\Omega = 0$ and $\Omega = -1$, respectively

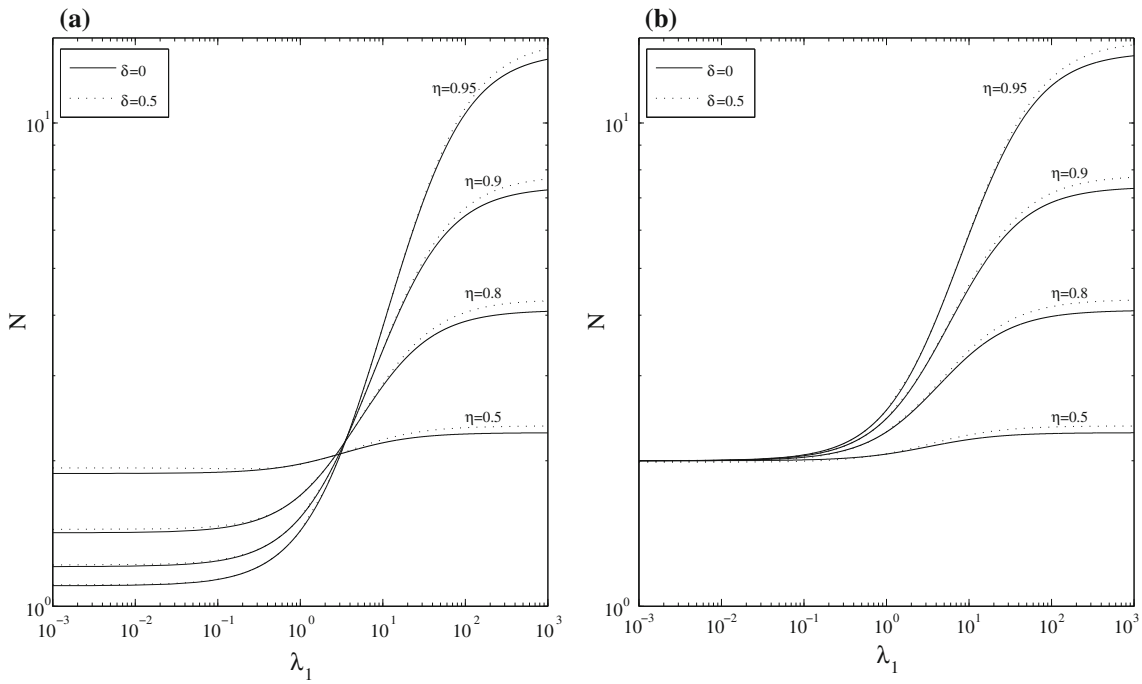

FIG. 6. Variations of the coupling coefficient with the parameter λ_1 for different values of the ratios η and δ with $\Omega = -1$. **a** and **b** represent the calculations for the $\lambda_2 = \lambda_1$ and $\lambda_2 \to \infty$, respectively

TABLE 1. *The coupling coefficient for the rotational motion of a spherical particle in a spherical container with* $\lambda_2 = \lambda_1$ *at various values of* δ, η *and* λ_1 *with* $\Omega = -1$

δ	η	N					
		$\lambda_1 = 0$	$\lambda_1 = 2$	$\lambda_1 = 3$	$\lambda_1 = 4$	$\lambda_1 = 10$	$\lambda_1 \to \infty$
10E-5	0.1	1.999800	2.000680	2.000901	2.001058	2.001493	2.002002
	0.2	1.996805	2.004490	2.006421	2.007802	2.011636	2.016129
	0.3	1.983930	2.011951	2.019080	2.024204	2.038528	2.055498
	0.4	1.950078	2.020692	2.039152	2.052545	2.090570	2.136752
	0.5	1.882353	2.025316	2.064516	2.093458	2.178010	2.285714
	0.6	1.770538	2.017431	2.090301	2.145660	2.315475	2.551020
	0.7	1.612773	1.986373	2.108481	2.205315	2.526651	3.044140
	0.8	1.418842	1.921303	2.107926	2.265079	2.854383	4.098361
	0.9	1.207657	1.814783	2.075658	2.313170	3.386166	7.380072
	0.99	1.020098	1.683164	2.009750	2.333103	4.207938	67.337860
0.25	0.1	1.999988	2.000756	2.001018	2.001205	2.001728	2.002340
	0.2	1.998699	2.004742	2.006932	2.008519	2.012976	2.018250
	0.3	1.989114	2.012261	2.020036	2.025708	2.041792	2.061109
	0.4	1.958851	2.020750	2.040293	2.054675	2.096113	2.147250
	0.5	1.893480	2.024809	2.065408	2.095746	2.185635	2.302197
	0.6	1.781703	2.016288	2.090583	2.147543	2.324467	2.574712
	0.7	1.621674	1.984925	2.108119	2.206399	2.535811	3.077403
	0.8	1.424274	1.920154	2.107306	2.265373	2.861978	4.147735
	0.9	1.209825	1.814355	2.075328	2.313114	3.390026	7.473525
	0.99	1.020257	1.683159	2.009745	2.333101	4.208023	68.202835
0.5	0.1	2.000464	2.001130	2.001583	2.001914	2.002846	2.003951
	0.2	2.004128	2.005848	2.009127	2.011585	2.018705	2.027375
	0.3	2.007127	2.013316	2.023524	2.031317	2.054414	2.083400
	0.4	1.990595	2.020730	2.043994	2.061908	2.116052	2.186576
	0.5	1.933053	2.022922	2.068029	2.103052	2.211673	2.361423
	0.6	1.820321	2.012527	2.091219	2.153298	2.354000	2.657499
	0.7	1.651631	1.980398	2.106860	2.209604	2.564972	3.191625
	0.8	1.442132	1.916659	2.105384	2.266209	2.885541	4.315584
	0.9	1.216828	1.813067	2.074332	2.312938	3.401743	7.789656
	0.99	1.020764	1.683143	2.009730	2.333093	4.208276	71.124802

N is much greater than that of the case when the particle and envelope rotate in the same direction ($\Omega > 0$) for the different values of δ, η. It is also noted that when the relative angular velocity is greater than unity ($\Omega > 1$), N becomes negative, indicating a reversal in the direction of the coupling coefficient for various values of δ, η. When the particle and envelope rotate with the same angular velocity in the same direction ($\Omega = 1$), the coupling coefficient vanishes ($N = 0$). Figure 5 shows the variation of the coupling coefficient as a function of the relative ratio of the radii for the values of $\delta = 0, 0.5$, which shows that N increases monotonically with the increase in δ when the other parameters are fixed. As expected, it is observed that N has its minimal value when the particle is in concentric position inside the envelope ($\delta = 0$). Figure 6 shows the variation of the coupling coefficient as a function of the slip parameter of the particle for different values of η, δ. There is an insignificant variation in the coupling coefficient between the plotted values of $\delta = 0$ and $\delta = 0.5$ for fixed η.

In general, the results in Tables 1, 2 and 3 and Figs. 2, 3, 4, 5 and 6 show that the couple coefficient N exerted on the particle in container increases monotonically with an increase in η for any given values of Ω, λ_1, λ_2 and δ. Also, this coefficient increases monotonically with an increase in δ, for any fixed values of Ω, λ_1, λ_2 and η. The coupling coefficient acting on the particle, in general, increases as λ_1 and λ_2 are increasing with keeping the other parameters unchanged. It has been found that our collocation results of N in the concentric limit of $\delta \to 0$ (given in the Tables 1, 2 and Figs. 4, 5 and 6) agree excellently with the analytical solution (3.8).

TABLE 2. *The coupling coefficient for the rotational motion of a spherical particle in a spherical container with $\lambda_2 \to \infty$ at various values of δ, η and λ_1 with $\Omega = -1$.*

δ	η	N			
		$\lambda_1 = 0$	$\lambda_1 = 1$	$\lambda_1 = 10$	$\lambda_1 \to \infty$
10E-5	0.1	2.000000	2.000500	2.001540	2.002002
	0.2	2.000000	2.004008	2.012384	2.016129
	0.3	2.000000	2.013592	2.042419	2.055498
	0.4	2.000000	2.032520	2.103560	2.136752
	0.5	2.000000	2.064516	2.212766	2.285714
	0.6	2.000000	2.114165	2.398524	2.551020
	0.7	2.000000	2.187585	2.716823	3.044140
	0.8	2.000000	2.293578	3.299493	4.098361
	0.9	2.000000	2.445735	4.553415	7.380072
	0.99	2.000000	2.640525	7.885934	67.337860
0.25	0.1	1.999949	2.000546	2.001788	2.002340
	0.2	1.999493	2.004149	2.013890	2.018250
	0.3	1.998600	2.013864	2.046334	2.061109
	0.4	1.997568	2.032964	2.110711	2.147250
	0.5	1.996764	2.065125	2.223521	2.302197
	0.6	1.996517	2.114873	2.412815	2.574712
	0.7	1.996996	2.188268	2.734149	3.077403
	0.8	1.998097	2.294080	3.318531	4.147735
	0.9	1.999364	2.445939	4.569716	7.473525
	0.99	1.999992	2.640528	7.886964	68.202835
0.5	0.1	1.999783	2.000824	2.002988	2.003951
	0.2	1.997749	2.005072	2.020458	2.027375
	0.3	1.993196	2.014966	2.061819	2.083400
	0.4	1.988336	2.034201	2.137092	2.186576
	0.5	1.985233	2.066704	2.261285	2.361423
	0.6	1.984883	2.116769	2.461198	2.657499
	0.7	1.987476	2.190183	2.791142	3.191625
	0.8	1.992275	2.295540	3.379526	4.315584
	0.9	1.997450	2.446547	4.620350	7.789656
	0.99	1.999969	2.640537	7.890059	71.124802

4. Conclusion

In this work, a combined analytical/numerical solution procedure for the slow steady rotational motion of a slip spherical particle at an eccentric position in a viscous fluid within a slip spherical container is presented. The solid particle and the spherical container rotate with different angular velocities about an axis joining their centers. The results for the coupling coefficient acting on the particle indicate that the solution procedure converges rapidly, and accurate solutions can be obtained for various cases of the particle's relative slip coefficient, the separation distance between the particle and the container surface. As expected, the coupling coefficient is a monotonic increasing function of the ratio of particle-to-container radii for all cases and becomes infinite in the touching limit. For a constant ratio of radii, the coupling is minimal when the particle is located at the container center and increases monotonically with the relative distance between the centers of the particle and the container surface. The impact of the slip on the couple is substantial and cannot be ignored, and it is observed that for each a slip particle coefficient, the coupling coefficient is a monotonic function of the ratio of the particle-to-container radii. However, this monotonic function is not the same for each slip particle coefficient. That is, it may be either decreasing or increasing.

TABLE 3. *The coupling coefficient for the rotational motion of a spherical particle in a spherical container with* $\lambda_2 = \lambda_1 = 10$ *at various values of* δ, η *and* Ω.

δ	Ω	N			
		$\eta = 0.1$	$\eta = 0.3$	$\eta = 0.6$	$\eta = 0.9$
10E-5	−2	3.002240	3.057792	3.473212	5.079249
	−1.5	2.501867	2.548160	2.894343	4.232708
	−1	2.001493	2.038528	2.315475	3.386166
	−0.5	1.501120	1.528896	1.736606	2.539625
	0	1.000747	1.019264	1.157737	1.693083
	0.5	0.500373	0.509632	0.578869	0.846542
	1	0.000000	0.000000	0.000000	0.000000
	1.5	−0.500373	−0.509632	−0.578869	−0.846542
	2	−1.000747	−1.019264	−1.157737	−1.693083
0.25	−2	3.002591	3.062688	3.486700	5.085039
	−1.5	2.502160	2.552240	2.905583	4.237533
	−1	2.001728	2.041792	2.324467	3.390026
	−0.5	1.501296	1.531344	1.743350	2.542520
	0	1.000864	1.020896	1.162233	1.695013
	0.5	0.500432	0.510448	0.581117	0.847507
	1	0.000000	0.000000	0.000000	0.000000
	1.5	−0.500432	−0.510448	−0.581117	−0.847507
	2	−1.000864	−1.020896	−1.162233	−1.695013
0.5	−2	3.004269	3.081621	3.530999	5.102614
	−1.5	2.503558	2.568018	2.942499	4.252179
	−1	2.002846	2.054414	2.354000	3.401743
	−0.5	1.502135	1.540811	1.765500	2.551307
	0	1.001423	1.027207	1.177000	1.700871
	0.5	0.500712	0.513604	0.588500	0.850436
	1	0.000000	0.000000	0.000000	0.000000
	1.5	−0.500712	−0.513604	−0.588500	−0.850436
	2	−1.001423	−1.027207	−1.177000	−1.700871

Appendix A

The functions appearing in Eqs. (3.3) and (3.4) are defined by

$$a_{1n}(r,\theta) = \frac{1}{r_1 \sin\theta_1}\left[r^{-n-1} P_n^1(\cos\theta) + \mu\,\beta_1^{-1}\,(n+2)\,r^{-n-2}\,P_n^1(\cos\theta)\right], \tag{A.1}$$

$$b_{1n}(r,\theta) = \frac{1}{r_1 \sin\theta_1}\left[r^{n} P_n^1(\cos\theta) - \mu\,\beta_1^{-1}\,(n-1)\,r^{n-1}\,P_n^1(\cos\theta)\right], \tag{A.2}$$

$$a_{2n}(r,\theta) = \frac{1}{r_2 \sin\theta_2}\left[r^{-n-1} P_n^1(\cos\theta) - \mu\,\beta_2^{-1}\,(n+2)\,r^{-n-2}\,P_n^1(\cos\theta)\right], \tag{A.3}$$

$$b_{2n}(r,\theta) = \frac{1}{r_2 \sin\theta_2}\left[r^{n} P_n^1(\cos\theta) + \mu\,\beta_2^{-1}\,(n-1)\,r^{n-1}\,P_n^1(\cos\theta)\right]. \tag{A.4}$$

Appendix B

Rotation of a sphere in a concentric spherical container with slip surfaces

We now consider the steady flow of an incompressible viscous fluid between two concentric spheres of radii a and $b\,(b > a)$ in which the outer sphere is rotating with angular velocity Ω_2 about the z-axis and

the inner sphere is rotating with angular velocity Ω_1 about the same axis, where the fluid is allowed to slip at both the particle and container surfaces.

The aim in this section is to obtain the hydrodynamic couple acting on the particle in the presence of the container. The fluid flow between the particle and the container is still governed by Eqs. (2.2) and (2.3), respectively, in spherical polar coordinates system (r, θ, ϕ) with the origin at the center of the particle. They must be solved subject to the following boundary conditions resulting from the slip boundary conditions at the particle and container surfaces:

On the particle surface $r = 1$

$$q_\phi = \Omega_1 \, a \, r \, \sin\theta + \beta_1^{-1} \, t_{r\phi}, \tag{B.1}$$

On the container surface $r = \eta^{-1}$

$$q_\phi = \Omega_2 \, a \, r \, \sin\theta - \beta_2^{-1} \, t_{r\phi}, \tag{B.2}$$

Here, $t_{r\phi}(r, \theta)$ is the shear stress,

$$t_{r\phi}(r, \theta) = \mu \, r \, \frac{\partial}{\partial r}\Big(\frac{q_\phi}{r}\Big). \tag{B.3}$$

A suitable solution of Eq. (2.2) as in [29] is

$$q_\phi = \Omega_1 \, a \left(A \, r^{-2} + B \, r\right) P_1^1(\cos\theta), \tag{B.4}$$

where A and B are arbitrary constants to be determined from the above boundary conditions (B.1) and (B.2). Thus, we have

$$A = \frac{\lambda_1 \, \lambda_2 \, (1 - \Omega)}{3\eta^4 \, \lambda_1 + (3 + \lambda_1 - \lambda_1 \, \eta^3) \, \lambda_2}, \tag{B.5}$$

$$B = 1 - \frac{(\lambda_1 + 3) \, \lambda_2 \, (1 - \Omega)}{3\eta^4 \, \lambda_1 + (3 + \lambda_1 - \lambda_1 \, \eta^3) \, \lambda_2}. \tag{B.6}$$

The hydrodynamic couple acting on the particle is found to be

$$T_z = -8 \, \pi \, \mu \, \Omega_1 \, a^3 \, A = \frac{-8 \, \pi \, \mu \, \Omega_1 \, a^3 \, \lambda_1 \, \lambda_2 \, (1 - \Omega)}{3\eta^4 \, \lambda_1 + (3 + \lambda_1 - \lambda_1 \, \eta^3) \, \lambda_2}. \tag{B.7}$$

The couple on the spherical container is equal and opposite to the value given by (B.7). Here, note that if we consider the limiting case $\lambda_i \to \infty$, which corresponds to the no-slip conditions on the sphere and container surfaces, the value of the couple is obtained explicitly as [2,13]

$$T_z = \frac{-8 \, \pi \, \mu \, \Omega_1 \, a^3 \, (1 - \Omega)}{1 - \eta^3}. \tag{B.8}$$

When $b \to \infty$, $\Omega = 0$ (or $\eta = 0$, $\Omega_2 = 0$), we recover the well-known result for the classic expression for the couple exerted by the ambient fluid on a rotating rigid sphere with a slip-flow boundary condition at its surface, first derived by Basset [29], as

$$T_z^\infty = \frac{-8 \, \pi \, \mu \, \Omega_1 \, a^3 \, \lambda_1}{\lambda_1 + 3}. \tag{B.9}$$

In the limiting case of the slip parameter $\lambda_1 = 0$, there is a perfect slip at the particle surface, and the hydrodynamic couple vanishes.

References

1. Pedlosky, J.: Axially symmetric motion of a stratified, rotating fluid in a spherical annulus of a narrow gape. J. Fluid Mech. **36**, 401–415 (1969)
2. Happel, J., Brenner, H.: Low Reynolds Number Hydrodynamics. Nijhoff, Dordrecht, The Netherlands (1983)
3. Nakabayashi, K., Tsuchida, Y.: Basic study on classification of fine particles in almost rigidly rotating flow (2nd report, dependence of Ekman layer and interior region on wall configuration of housing and rotor. Trans. Jpn. Soc. Mech. Eng. B **61**(591), 3996–4003 (1995)
4. Nakabayashi, K., Tsuchida, Y., Takeo, K., Ono, Y.: Basic study on classification of fine particles in almost rigidly rotating flow (3rd report, conditions of occurrence of a stable regime of almost rigidly rotating flow. Trans. Jpn. Soc. Mech. Eng. B **61**(591), 4004–4010 (1995)
5. Lee, E., Huang, Y.F., Hsu, J.P.: Electrophoresis in a non-Newtonian fluid: sphere in a spherical cavity. J. Colloid Interface Sci. **258**, 283–288 (2003)
6. Lee, E., Ming, J.K., Hsu, J.P.: Purely viscous flow of a shear-thinning fluid between two rotating spheres. Chem. Eng. Sci. **59**, 417–424 (2004)
7. Lamb, H.: Hydrodynamics, 6th edn. Cambridge University Press, Cambridge (1932)
8. Jeffery, G.B.: Steady rotation of a solid of revolution in a viscous fluid. Proc. Lond. Math. Soc. **14**, 327–338 (1915)
9. Kanwal, R.P.: Steady rotation of axially symmetric bodies in a viscous fluid. J. Fluid Mech. **10**, 17–24 (1960)
10. Wakiya, S.: Slow motion around two spheres. J. Phys. Soc. Jpn. **22**, 1101–1109 (1967)
11. O'Neill, M.E.: Exact solutions of the equations of slow viscous flow generated by the asymmetrical motion of two spheres. Appl. Sci. Res. **21**, 452–466 (1969)
12. Nir, A., Acrivos, A.: On the creeping of two arbitrary-sized touching spheres in a linear shear field. J. Fluid Mech. **59**, 209–223 (1973)
13. Landau, L.D., Lifshitz, E.M.: Course of theoretical physics, vol. 6. Fluid Mechanics Pergamon Press, Pergamon (1959)
14. Munson, B.R., Joseph, D.D.: Viscous incompressible flow between concentric rotating sphere, Part 1. Basic flow. J. Fluid Mech. **49**, 289–303 (1971)
15. Munson, B.R.: Viscous incompressible flow between eccentric coaxially rotating spheres. Phys. Fluids **17**, 528–531 (1974)
16. O'Neill, M.E., Majumdar, S.R.: Asymmetrical slow viscous fluid motions caused by the translation or rotation of two spheres-part I: the determination of exact solutions for any values of the ratio of radii and separation parameters. J. Appl. Math. Phys. (ZAMP) **21**, 164–179 (1970)
17. O'Neill, M.E., Majumdar, S.R.: Asymmetrical slow viscous fluid motions caused by the translation or rotation of two spherespart II: asymptotic forms of the solutions when the minimum clearance between the spheres approaches zero. J. Appl. Math. Phys. (ZAMP) **21**, 180–187 (1970)
18. Cooley, M.D.A.: The slow rotation in a viscous fluid of a sphere close to another fixed sphere about a diameter perpendicular to the line of centers. Quart. J. Mech. Appl. Math. **24**, 237–250 (1971)
19. Kamel, M.T., ChanMan Fong, C.F.: Micropolar fluid flow between two eccentric coaxially rotating spheres. Act. Mech. **99**, 155–171 (1993)
20. Srivastava, D.K.: Slow rotation of concentric spheres with source at their centre in a viscous fluid. J. Appl. Math. (2009) doi:10.1155/2009/740172
21. Shankar, P.N.: Exact solutions for Stokes flow in and around a sphere and between concentric spheres. J. Fluid Mech. **631**, 363–373 (2009)
22. Jabari Moghadam, A., Rahimi, A.B.: A numerical study of flow and heat transfer between two rotating spheres with time-dependent angular velocities. J. Heat Transf. **130**, 071703 (2008)
23. Liu, Q., Prosperetti, A.: Wall effects on a rotating sphere. J. Fluid Mech. **657**, 1–21 (2010)
24. Keh, H.J., Lee, T.C.: Axisymmetric creeping motion of a slip spherical particle in a nonconcentric spherical cavity. Theor. Comput. Fluid Dyn. **24**, 497–510 (2010)
25. Kennard, E.H.: Kinetic Theory of Gases. McGraw-Hill, New York (1938)
26. Hutchins, D.K., Harper, M.H., Felder, R.L.: Slip correction measurements for solid spherical particles by modulated dynamic light scattering. Aerosol. Sci. Technol. **22**, 202–218 (1995)
27. Thompson, P.A., Troian, S.M.: A general boundary condition for liquid flow at solid surfaces. Nature **389**, 360–362 (1997)
28. O'Neill, M.E., Ranger, K.B., Brenner, H.: Slip at the surface of a translating-rotating sphere bisected by a free surface bounding a semi-infinite viscous fluid: removal of the contact-line singularity. Phys. Fluids **29**, 913–924 (1986)
29. Basset, A.B.: A Treatise on Hydrodynamics, Vol. 2, pp. 247–248. Dover, New York (1961)
30. Navier, C.L.M.H.: Memoirs de l'Academie Royale des Sciences de l'Institut de France, vol. 1, pp. 414-416 (1823)
31. Keh, H.J., Chang, J.H.: Boundary effects on the creeping-flow and thermophoretic motions of an aerosol particle in a spherical cavity. Chem. Eng. Sci. **53**, 2365–2377 (1998)
32. Tekasakul, P., Tompson, R.V., Loyalka, S.K.: A numerical study of two coaxial axi-symmetric particles undergoing steady equal rotation in the slip regime. J. Appl. Math. Phys. (ZAMP) **50**, 387–403 (1999)

33. Neto, C., Evans, D.R., Bonaccurso, E., Butt, H.-J., Craig, V.S.J.: Boundary slip in Newtonian liquids: a review of experimental studies. Rep. Progr. Phys. **68**, 2859–2897 (2005)
34. Suna, H., Liu, C.: The slip boundary condition in the dynamics of solid particles immersed in Stokesian flows. Solid State Commun. **150**, 990–1002 (2010)
35. Yang, F.: Slip boundary condition for viscous flow over solid surfaces. Chem. Eng. Commun. **197**, 544–550 (2010)
36. Sherief, H.H., Faltas, M.S., Saad, E.I.: Slip at the surface of a sphere translating perpendicular to a plane wall in micropolar fluid. J. Appl. Math. Phys. (ZAMP) **59**, 293–312 (2008)
37. Sherief, H.H., Faltas, M.S., Ashmawy, E.A.: Galerkin representations and fundamental solutions for an axisymmetric microstretch fluid flow. J. Fluid Mech. **619**, 277–293 (2009)
38. Whitmer, J.K., Luijten, E.: Fluid-solid boundary conditions for multiparticle collision dynamics. J. Phys. Condens. Matter **22**, 104106 (2010)
39. Gluckman, M.J., Pfeffer, R., Weinbaum, S.: A new technique for treating multiparticle slow viscous flow: axisymmetric flow past spheres and spheroids. J. Fluid Mech. **50**, 705–740 (1971)
40. Leichtberg, S., Pfeffer, R., Weinbaum, S.: Stokes flow past finite coaxial clusters of spheres in a circular cylinder. Int. J. Multiph. Flow **3**, 147–169 (1976)
41. Ganatos, P., Weinbaum, S., Pfeffer, R.: A strong interaction theory for the creeping motion of a sphere between plane parallel boundaries. Part 1. Perpendicular motion. J. Fluid Mech. **99**, 739–753 (1980)
42. Ganatos, P., Weinbaum, S., Pfeffer, R.: A strong interaction theory for the creeping motion of a sphere between plane parallel boundaries. Part 2. Parallel motion. J. Fluid Mech. **99**, 755–783 (1980)
43. Lu, S.Y., Lee, C.T.: Boundary effects on creeping motion of an aerosol particle in a non-concentric pore. Chem. Eng. Sci. **56**, 5207–5216 (2001)
44. Chen, P.Y., Keh, H.J.: Slow motion of a slip spherical particle parallel to one or two plane walls. J. Chin. Inst. Chem. Eng. **34**, 123–133 (2003)
45. Lu, S.Y., Lee, C.T.: Creeping motion of a spherical aerosol particle in a cylindrical pore. Chem. Eng. Sci. **57**, 1479–1484 (2002)
46. Faltas, M.S., Saad, E.I.: Stokes flow past an assemblage of slip eccentric spherical particle-in-cell models. Math. Methods Appl. Sci. **34**, 1594–1605 (2011)
47. Bocquet, L., Barrat, J.-L.: Flow boundaries from nano- to micro-scales. Soft Matter **3**, 685–693 (2007)

M. S. Faltas
Department of Mathematics
Faculty of Science
Alexandria University
Alexandria
Egypt

E. I. Saad
Department of Mathematics
Faculty of Science
Damanhour University
Damanhour
Egypt
e-mail: elsayedsaad74@yahoo.com

(Received: April 6, 2011; revised: September 16, 2011)